# An effect of the aspect ratio on the ultimate strength of lean duplex stainless steel outstanding plate element

Kensuke NISHIDA* and Takao MIYOSHI*

**ABSTRACT**

The material cost of recently developed lean duplex stainless steel JIS SUS821L1 is lower than that of austenitic stainless steel JIS SUS304 which is most commonly used stainless steel in Japan. Although SUS821L1 has far lower nickel content in comparison with SUS304, its corrosion resistance is equivalent to SUS304. For this reason, SUS821L1 contributes to reducing the initial material cost of infrastructures as well as the maintenance cost for their repainting. This study focuses on the application of SUS821L1 to I-section main-girder of the small-scale bridges. It is required to fabricate by welding, because SUS821L1 hot rolled H-beams has not been produced yet in Japan. Therefore, it consists of the welded outstanding plate element. This study aims to clarify an effect of the aspect ratio on the ultimate strength of SUS821L1 welded outstanding plate element under uniaxial compression. In order to investigate the compression behavior and the ultimate strength, parametric studies regarding plate slenderness parameter, aspect ratio and welding residual stress are carried out using finite element (FE) analysis. Numerical results are compared with design strength and maximum plate width to thickness ratio specified in existing design standard. Based on the comparison, the applicability of design curve and limiting plate width to thickness ratio for yielding are clarified.

**KEY WORDS**: Lean duplex stainless steel, outstanding plate element, aspect ratio, welding residual stress, ultimate strength

## 1. Introduction

There are few structural applications of the stainless steel in Japan, because it is an expensive construction material. However, recently, high durability and long service life of infrastructures are generally required in Japan, and contribution of the stainless steel to enhancement of the environmental performance has widely become known, too[1]. Therefore, a trend toward application of the stainless steel to infrastructures is growing. In Japan, stainless steel has already been used for some waterside structures, such as dam, gate etc. which are in severe corrosion environment[2), 3)]. Also, Japan's first duplex stainless steel bridge was constructed in 2017[4]. In Japan specifications for highway bridges (JSHB)[5], which was drastically revised in November 2017, it is specified that the service life of the bridge is a hundred years. Additionally, load and resistance factored design method (LRFD) is introduced into JSHB instead of allowable design method (ASD), which was adopted in its previous version, so that new material or structure which contribute to enhancing durability or prolonging service life of the bridge are able to be applied to it easily. For this reason, positive research activities for structural application of the stainless steel have already begun in Japan[6].

The main difficulty to apply stainless steel to infrastructures is its high material cost that is affected by its nickel content. Austenitic grade JIS SUS304, which is most commonly adopted in stainless steel family, has around 8 % nickel content. Therefore, bridges using SUS304 have never been constructed in Japan. However, the recently developed lean

*Department of civil engineering

duplex stainless steel has around 1.5 % nickel content. Despite the low nickel content, its corrosion resistance is similar to that of SUS304. SUS821L1 was standardized under JIS G 4304: 2015 as a lean duplex stainless steel in Japan[7]. The initial material cost of SUS821L1 is relatively low within stainless steels because of its low nickel content. Consequently, structural application of SUS821L1 to infrastructures contributes to reducing of their life cycle cost, laborsaving of their maintenance work and achieving their long service life. In order to make it widespread, it is necessary to verify its productivity, workability and durability by applying it to I-section main-girder of the small-scale bridges, as shown in Fig.1. For the purpose of it, load carrying capacity of I-section main-girder has to be clarified. Existing studies on structural behavior of SUS821L1 have been reported with regard to the stress-strain relationship, residual stresses and geometric imperfections of the welded I-section[8), 9)], ultimate strength of the plate elements[10)], welded H-section stub-columns[11)] and welded I-section subjected to pure bending[12)]. However, there are few studies on an effect of the aspect ratio on the ultimate strength of SUS821L1 outstanding plate element.

This study aims to investigate an effect of the aspect ratio on the compression behavior and the ultimate strength of SUS821L1 outstanding plate element. Parametric studies regarding plate slenderness parameter, aspect ratio and welding residual stress were carried out to assess compression behavior and ultimate strength using FEM computer program. Numerical results were compared with the ultimate strength and maximum plate width to thickness ratio specified in existing design standards[5), 13)].

## 2. Investigation method

Elasto-plastic finite displacement analysis was performed using an FEM program developed by authors. Eight-node isoparametric shell element is involved in the element library of this program. As a material model of stainless steel, MRO curve is incorporated into the program. Von mises yield function, associated flow rule and implicit stress integration scheme are employed to treat elasto-plastic problem, and updated Lagrangian formulation is applied to consider geometric nonlinearity. This program was verified by comparing the numerical results with test results of welded H-section stub-columns[11)].

### 2・1 Stress-strain model of SUS821L1

Compression/tension coupon tests of SUS821L1 hot-rolled

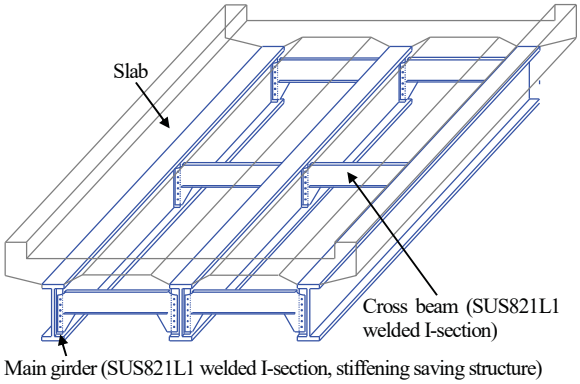


Fig.1 Schematic drawing of the small-scale bridge

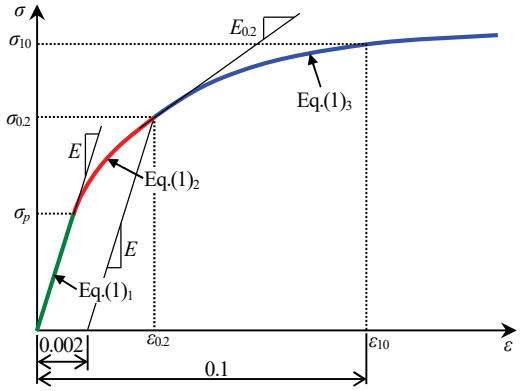


Fig.2 Schematic drawing of MRO curve

plate in longitudinal and transverse direction were carried out and the applicability of MRO curve to SUS821L1 was verified by comparing test results with the curve. As a result, it was shown that MRO curve is good agreement with test results[8), 9)]. As shown in Fig. 2, this curve is a linear elastic body up to the proportion limit $\sigma_p$, and two Ramberg-Osgood curves are connected smoothly at material 0.2% proof stress $\sigma_{0.2}$ after $\sigma_p$, as expressed by eqs.(1) and (2).

$$\varepsilon=\begin{cases}\dfrac{\sigma}{E} & \left(0\le\sigma<\sigma_p\right)\\ \dfrac{\sigma}{E}+a_m\left(\sigma^{n1}-\sigma_p^{n1}\right) & \left(\sigma_p\le\sigma<\sigma_{0.2}\right)\\ \dfrac{\sigma}{E}+b_m\sigma+c_m+d_m\left(\sigma-\sigma_{0.2}\right)^{n1} & \left(\sigma_{0.2}\le\sigma\right)\end{cases} \quad (1)_{1\text{-}3}$$

$$a_m=\frac{0.002}{\sigma_{0.2}^{n1}-\sigma_p^{n1}},\ b_m=\frac{0.002n1\sigma_{0.2}^{n1-1}}{\sigma_{0.2}^{n1}-\sigma_p^{n1}},$$

$$c_m=\varepsilon_{0.2}-\frac{\sigma_{0.2}}{E_{0.2}}, \quad (2)_{1\text{-}4}$$

$$d_m=\frac{1}{\left(\sigma_{10}-\sigma_{0.2}\right)^{n2}}\left(\varepsilon_{10}-\varepsilon_{0.2}-\frac{\sigma_{10}-\sigma_{0.2}}{E_{0.2}}\right),$$

$$E_{0.2}=\frac{E\left(\sigma_{0.2}^{n1}-\sigma_p^{n1}\right)}{\sigma_{0.2}^{n1}-\sigma_p^{n1}+0.002n1E\sigma_{0.2}^{n1-1}}$$

where $\varepsilon$ is the strain, $\sigma$ is the stress, $E$ is the modulus of

elasticity, $\sigma_p$ is the proportion limit, $n1$ and $n2$ are strain hardening exponents of the first and second curves, respectively, $\sigma_{0.2}$ is the material 0.2% proof stress, $\varepsilon_{0.2}$ is the strain at $\sigma_{0.2}$, $\varepsilon_{10}$ is the 10% strain (= 0.1), $\sigma_{10}$ is the stress at 10% strain.

Based on the existing study on compressive strength of SUS821L1 outstanding plate with 4.0 in aspect ratio[10], values obtained from the existing coupon test results[8), 9)] of transverse direction were employed as material constants of the model, as shown in Table 1.

### 2・2 Parametric studies

Numerical simulations on a total of 84 SUS821L1 outstanding plate elements subjected to uniform compression were carried out, incorporating a wide range of web slenderness parameter $\lambda_p$ (0.5, 0.7, 0.9, 1.1, 1.3 and 1.5), aspect ratio $\alpha$ (0.5, 1.0, 2.0, 3.0, 4.0, 5.0 and 6.0) and existence of residual stress. $\lambda_p$ and $\alpha$ are are given by Eqs. (3) and (4), respectively.

$$\lambda_p = \frac{b}{t}\sqrt{\frac{12\left(1-\nu^2\right)}{k\pi^2}\frac{\sigma_{0.2}}{E}} \qquad (3)$$

$$\alpha = \frac{a}{b} \qquad (4)$$

where $b$ is the plate width, $t$ is the plate thickness, $k$ is the buckling coefficient (assumed as a constant value of 0.43), $a$ is the length of the side edge. Symbols for geometry of the outstanding plate element are defined in Fig.3.

Maximum value of $\lambda_p$ was based on the maximum plate width to thickness ratio of outstanding plate $b/t$ = 16 which is specified in JSHB[14], and material properties shown in Table 1. On the other hand, minimum value of $\lambda_p$ was determined from existing study[15], because the ultimate compressive strength of the carbon steel outstanding plate exceeds yield strength at $\lambda_p$ = 0.5.

FE model of the outstanding plate subjected to uniform compression were considered its symmetry, as shown in Fig.3.

### 2・3 Residual stresses

Residual stress distribution model for welded duplex stainless steel structure which is proposed by Gardner[16] was employed, as shown in Fig.3, because the model is good agreement with measured residual stress distribution and is able to be modeled easily by practical finite element division. Compressive residual stress $\sigma_{rc}$ is represented by Eq. (5).

$$\sigma_{rc} = \frac{a_1 + a_2}{2b - (a_1 + a_2)}\sigma_{rt} \qquad (5)$$

Table 1 Material constants of MRO curve and Poisson's ratio

| $\nu$ | $E$ (N/mm$^2$) | $\sigma_p$ (N/mm$^2$) | $\sigma_{0.2}$ (N/mm$^2$) | $E_{0.2}$ (N/mm$^2$) | $\sigma_1$ (N/mm$^2$) | $\sigma_{10}$ (N/mm$^2$) | $n_1$ | $n_2$ |
|---|---|---|---|---|---|---|---|---|
| 0.24 | 212708 | 388 | 577 | 31117 | 627 | 723 | 7.52 | 2.43 |

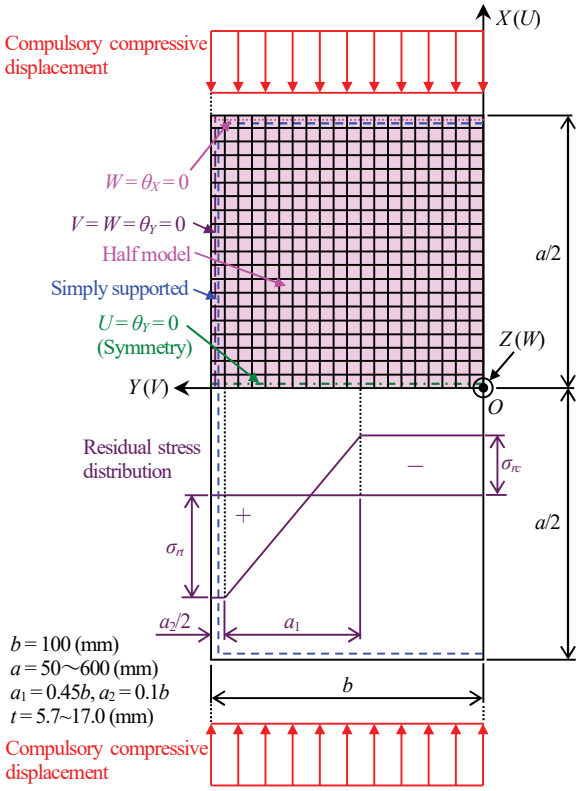


Fig.3 FE model of the outstanding plate element

where $\sigma_t$ is the maximum value of the tensile residual stress ($0.6\sigma_{0.2}$ is used for duplex stainless steel), $a_1$, $a_2$ are distribution width, as shown in Fig.3, respectively.

### 2・4 Initial geometric imperfections

Based on the existing study[15], the shape of the initial geometric imperfection was assumed as Eq.(6).

$$w_0 = w_{0\max}\left(1-\frac{Y}{b}\right)\cos\left(\frac{\pi}{a}X\right) \qquad (6)$$

where $w_{0max}$ is the maximum value of the initial geometric imperfection given by Eq.(7) which is specified in JSHB[14] as perpendicularity of flange.

$$w_{0\max} = \frac{b}{100} \qquad (7)$$

## 3. Numerical results

### 3・1 Load versus displacement curves

Figs.4-6 show load versus displacement curves for $\lambda_p$ = 0.7, 1.1, and 1.5 with residual stress, respectively. In these figures, the vertical axis indicates the non-dimensional parameter of

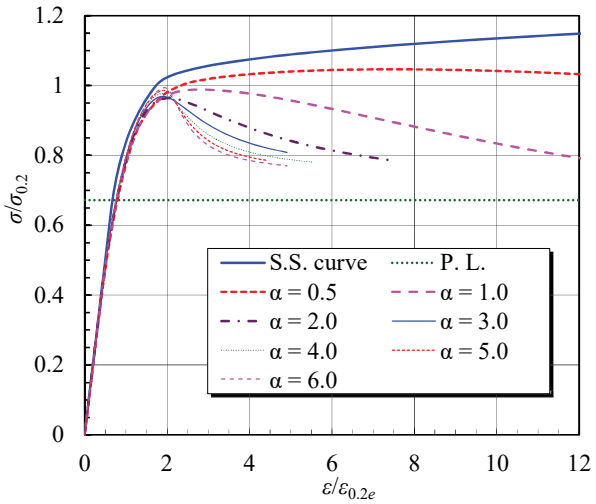


Fig.4 Load-displacement curves ($\lambda_p = 0.7$, with R.S.)

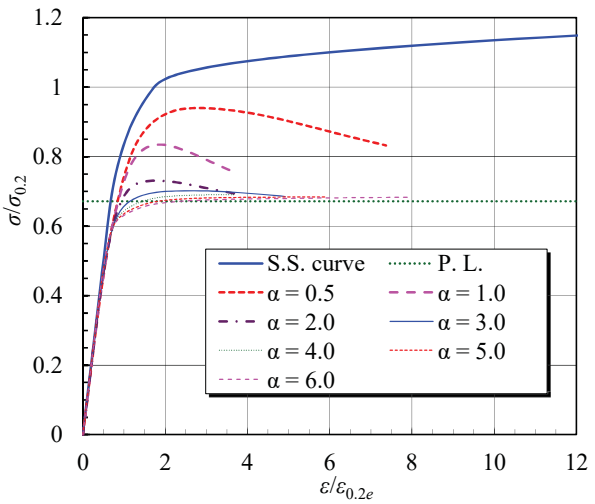


Fig.5 Load-displacement curves ($\lambda_p = 1.1$, with R.S.)

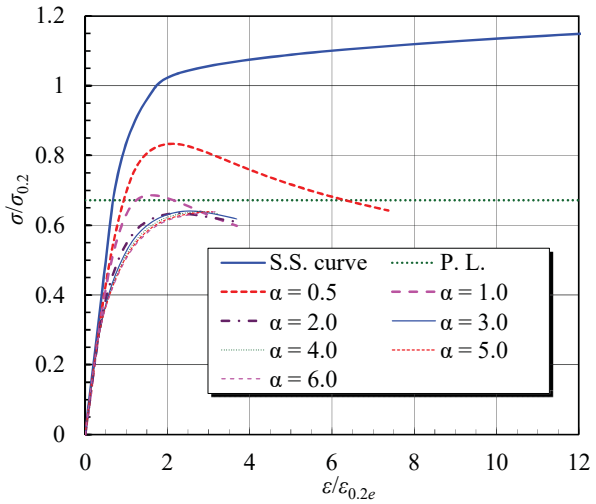


Fig.6 Load-displacement curves ($\lambda_p = 1.5$, with R.S.)

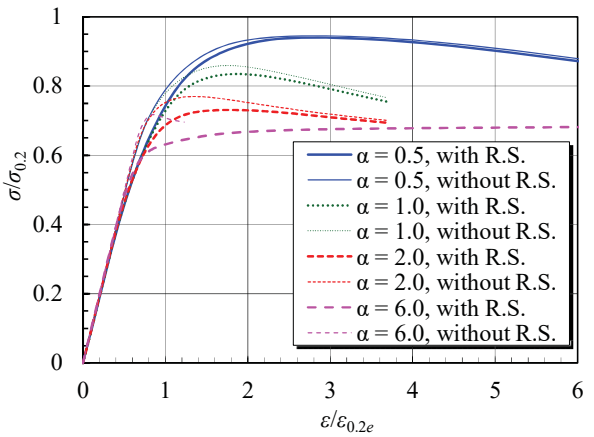


Fig.7 Effect of residual stress on load-displacement curves ($\lambda_p = 1.1$)

compressive stress $\sigma$ divided by $\sigma_{0.2}$ and the lateral axis denotes the non-dimensional parameter of average compressive strain $\varepsilon$ divided by $\varepsilon_{0.2e}$, where $\varepsilon_{0.2e}$ is the elastic strain at 0.2% proof stress. “R. S.” means residual stress. Also, non-dimensional stress-strain curve (S.S. curve) and proportion limit (P. L.) $\sigma_p$ are shown in the figures.

Figs.4–6 show that SUS821L1 welded outstanding plate elements exhibit a smooth curve up to the peak point because of the rounded stress-strain curve.

From Fig.4, ultimate strength of plate element with $\lambda_p = 0.7$ decreases gradually with an increase of $\alpha$. Also, the stiffness up to the peak point is almost similar, whereas reduction of the stiffness in post-peak becomes greater with an increase in the $\alpha$ value.

From Fig.5, the ultimate strength of plate element with $\lambda_p = 1.1$ decreases with an increase in the $\alpha$ value. Although decrease of the ultimate strength is drastically from 0.5 to 2.0 in the $\alpha$ value, the ultimate strength of the plates with $\alpha \geq 2.0$ are almost same. All plate elements exhibit non-linear behavior after average compressive stress attains around proportion limit.

From Fig.6, plate elements with $\lambda_p = 1.5$ exhibit a tendency similar to ones with $\lambda_p = 1.1$. However, the stiffness of plate elements with $\alpha \geq 3.0$ decreases rapidly with an increase of compressive stress.

Fig.7 shows the effect of residual stress on load versus displacement curves for $\lambda_p = 1.1$ and $\alpha = 0.5$, 1.0, 2.0 and 6.0. From this figure, it is shown that load versus displacement curves for $\alpha = 0.5$ and 1.0 are not influence by residual stress. However, load versus displacement curves for $\alpha = 2.0$ and 6.0 exhibit gradual yielding owing to residual stress.

### 3・2　Ultimate strength

Fig.8 shows the relationship between the ultimate strength and the aspect ratio $\alpha$. From this figure, regardless of residual

stress, the ultimate strength generally decreases with an increase in the $\alpha$ value. However, as for the ultimate strength, there are no significant differences from 4.0 to 6.0 in the $\alpha$ value. Therefore, in practice, the ultimate strength of SUS821L1 outstanding plate is able to be conservatively evaluated using that of one with $\alpha = 4.0$.

### 3・3 Comparison FE results with design curves

To discuss the applicability of the design strength curves provided in several design standards to welded SUS821L1 outstanding plate element, Fig.9 shows a comparison between ultimate strength obtained from FE results, Euler curve and design strength based on rules specified in JSHB[5] and Eurocode3 (EC3)[13]. In this figure, the vertical axis indicates the non-dimensional parameter of the ultimate stress $\sigma_u$ divided by $\sigma_{0.2}$.

From Fig.9, the ultimate strength of SUS821L1 plates with $\lambda_p = 0.7$ except for $\alpha = 0.5$ is greater than the design strength according to the JSHB curve, because this curve is used for carbon steel outstanding plate. As a result, this curve generally gives very conservative design strength for SUS821L1 plates with $\lambda_p \geq 0.9$. On the other hand, EC3 curve almost corresponds to the lower value of the ultimate strength, because this curve was proposed for stainless steel outstanding plate. Therefore, this curve is applicable to evaluate the ultimate strength rationally.

### 3・4 Limiting plate width to thickness ratio for yielding

Fig.10 shows the relationship between ultimate strength and plate width to thickness ratio $b/t$, including limiting plate width to thickness ratio for class 1-3 sections of welded duplex stainless steel plate element under uniaxial compression specified in EC3[13], where $b$ is the plate width and $t$ is the thickness.

This figure shows that the ultimate strength of SUS821L1 plates with $b/t < 7$ exceeds the yield strength. Consequently, maximum plate width to thickness ratio for class-2 section is able to be used for limiting plate width to thickness ratio for yielding of welded SUS821L1 outstanding plate elements.

## 4. Conclusions

In this study, an effect of the aspect ratio on the compression behavior and the ultimate strength of welded SUS821L1 outstanding plate element was evaluated through parametric studies using FEA. In addition, the design strength based on rules specified in existing design standards were compared with the ultimate strength based on

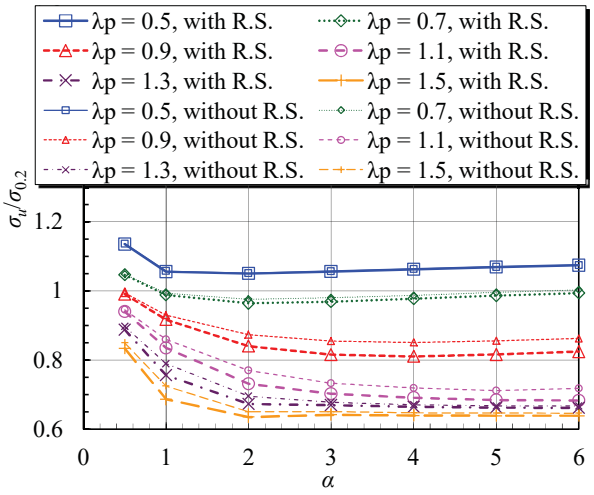


Fig.8 Influence of aspect ratio on ultimate strength

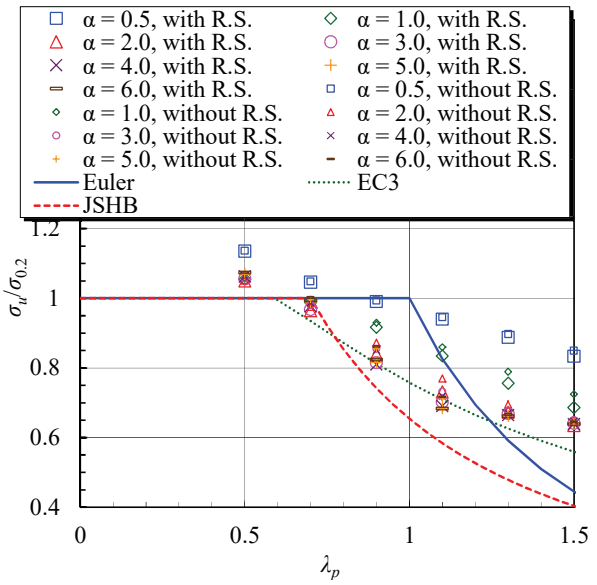


Fig.9 Comparison of FE results with design curves

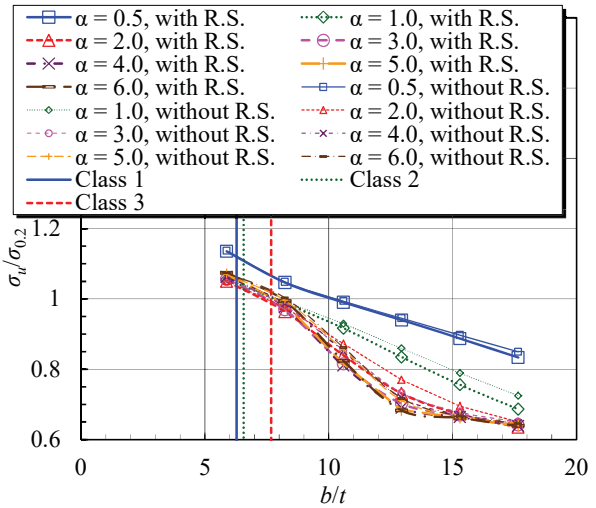


Fig.10 Comparison of FE results with maximum plate width to thickness ratio specified in EC3

numerical results. Furthermore, limiting plate width to

thickness ratio for yielding was discussed by compared with limiting plate width to thickness ratio specified in EC3[13]. The obtained results can be summarized as follows:

(1) The stiffness up to peak point of plate elements with aspect ratio from 0.5 to 2.0 decreases drastically.

(2) The effect of residuals stresses on the stiffness and the ultimate strength of plate elements with aspect ratio of 0.5 and 1.0 is very small.

(3) Regardless of residual stress, the ultimate strength generally decreases with an increase in the aspect ratio and the change of the ultimate strength with aspect ratio exceeding 4.0 exhibits considerably small.

(4) The design strength curve provided in the Japan specifications for highway bridges generally provide very conservative estimates of the ultimate strength of SUS821L1 welded outstanding plate element.

(5) The design strength curve specified in Eurocode3 almost corresponds to the lower value of the ultimate strength of SUS821L1 welded outstanding plate element.

(6) Maximum plate width to thickness ratio for class-2 section is able to be used for limiting plate width to thickness ratio for yielding of welded SUS821L1 outstanding plate elements.

**References**

1) T. Inada: Stainless steel for enhancement of the environmental performance, JSSC, No.15, pp.3-17, 2013. (in Japanese)

2) Japanese Society of Steel Construction: Special issue - A spread of the duplex stainless steel to structural application, JSSC, No.19, pp.3-21, 2014. (in Japanese)

3) N. Fukushima: An application of lean duplex stainless steel to selective withdrawal facility of Ninose dam, JSSC, No.29, pp.28-29, 2017. (in Japanese)

4) K. Yoshikawa: An application of stainless steel into Sumidagawa Terrace bridge in sluice gate of Kiyosu drainage pumping station, JSSC, No.33, pp.28-29, 2018. (in Japanese)

5) Japan Road Association: Specifications for highway bridges Part II Steel bridges and members, 2017. (in Japanese)

6) Japanese Society of Steel Construction, Committee on standardization of the stainless steel technique: Special issue - JSSC's now, heading towards more development and spread of stainless steel ~ for the purpose of standing committee activation, JSSC, No.30, pp.9-16, 2017. (in Japanese)

7) S. Tuge: Development and prospect of resource-saving type stainless steel which can replace common stainless steel, JSSC, No.33, pp.8-11, 2018. (in Japanese)

8) T. Miyoshi: Residual stresses of lean duplex stainless steel member with welded I-shaped sections, Proc. of 71st. annual meeting of JSCE, I-306, pp.611-612, 2016. (in Japanese)

9) T. Miyoshi: Mechanical properties and residual stresses of SUS821L1 welded I-section, Journal of Construction Steel, Vol.24, pp.305-312, 2016. (in Japanese)

10) T. Miyoshi: Effect of Stress-Strain Curve on Ultimate Compressive Strength of Lean Duplex Stainless Steel Plates, Memoirs of National Institute of Technology, Akashi College, Japan, No.59, pp.7-12, 2017. (in Japanese)

11) T. Miyoshi: An experimental study on the ultimate strength of lean duplex stainless steel H-shaped stub-columns, Journal of structural engineering, Vol.63A, pp.67-77, 2017. (in Japanese)

12) T. Miyoshi：Flexural Behavior of Lean Duplex Stainless Steel Welded I-section, Memoirs of National Institute of Technology, Akashi College, Vol.60, pp.1-8, 2018.

13) European Committee for Standardization, CEN : Eurocode3-Design of steel structures-part1-4 : General rules- Supplementary rules for stainless steels , EN 1993-1-4, 2006.

14) Japan Road Association: Specifications for highway bridges Part II Steel bridges, 2012. (in Japanese)

15) S. Komatsu and T. Kitada: Ultimate strength characteristics of outstanding steel plates with initial imperfections under compression, Proc. of JSCE, No.314, pp.15-27, 1981. (in Japanese)

16) H.X. Yuan, Y.Q. Wang, Y.J. Shi and L. Gardner : Residual stress distributions in welded stainless steel sections, Thin-Walled Structures, Vol.79, pp.38-51, 2014.